

Implementing VERSE for Time of Flight RF pulses at 7Tesla: Methodological Considerations

S. Schmitter¹, S. Johst², M. Bock², K. Ugurbil¹, and P-F. van de Moortele¹

¹University of Minnesota, Center for Magnetic Resonance Research, Minneapolis, MN, United States, ²German Cancer Research Center, Heidelberg, Germany

INTRODUCTION. In Time-of-flight (TOF) angiography, fresh blood inflowing spins provide bright intravascular signal while static tissue signal suppression is obtained in the steady state with $TR \ll T_1$. At 1.5 and 3T, stronger background suppression is achieved with magnetization transfer (MT), and venous contribution is attenuated with saturation RF pulses. Ramp shaped RF pulses (TONE) can be used to adjust blood velocity sensitivity. Successful TOF can be obtained at 7T, benefiting from higher SNR and longer tissue T_1 . However, because of SAR constraints, MT cannot be used at 7T and saturation pulses are often skipped [1-3]. SAR constraints also imply using sub-optimal excitation flip angle which in turn limits angiogram quality. These issues can be addressed using VERSE principle [4] to decrease peak RF power. However, VERSE pulses are more sensitive to ΔB_0 [4], while ΔB_0 increases proportionally with B_0 . Here, we investigate in simulations and in vivo the impact of off-resonance frequencies on RF excitation profile when applying VERSE at 7T.

MATERIAL AND METHODS. Measurements were performed at 7T (Siemens, Erlangen, Germany). **VERSE.** A VERSE algorithm [4] was implemented in the original TOF sequence. Initial TONE RF pulse shape $b_1(t)$ for medium flow and resulting VERSE RF $b_{1,v}(t)$ and gradient $g_v(t)$ pulse shapes are shown in Fig. 1. $g_v(t)$ and $b_{1,v}(t)$ are constrained to max RF amplitude, max gradient strength ($g_{max}=20\text{mT/m}$) and max slew rate ($s_{max}=100\text{T/m/s}$) with $g_v(t) \leq g_{max}$, $\partial g_v(t)/\partial t \leq s_{max}$, and $b_{1,v} \leq 0.3 \max[b_1(t)]$. The latter constraint limits the RF amplitude to $\kappa=30\%$ of its initial maximum value. By compressing low amplitude RF pulse segments (i.e. the sidelobes), a resulting pulse duration of 1.33 ms was achieved. **Simulations.** Excitation profiles were simulated with VERSE TONE pulses in Matlab (The MathWorks, Natick, USA) based on Bloch equations. Frequency offsets ($\pm 200\text{Hz}$) were introduced to evaluate the impact of susceptibility induced ΔB_0 . Offsets of -1000 Hz were used to evaluate water-fat chemical shift impact. Standard RF pulses (non TONE) were simulated for comparison. **Excitation profile.** Excitation profiles were measured in a phantom using an acquisition FOV along the slice direction 4 times larger than the excitation slab thickness. Imaging parameters were $TR/TE = 100\text{ms}/3.5\text{ms}$, $\alpha = 15\text{deg}$, slab/slice thickness: $16\text{mm}/0.5\text{mm}$, Matrix: $64 \times 64 \times 128$, $BW = 300\text{Hz/Px}$. To remove Receive B1 profile, $T2^*$ and Transmit B1 profile, these profiles were normalized with a 3D dataset acquired with same parameters but with a nonselective excitation (T_1 bias was minimal given the small flip angle). Residual timing errors between gradient and RF pulses were eliminated in calibration sessions. For in vivo measurements B_0 shimming was first performed with a single iteration and a field map was acquired ($TE/2 = 5.00/6.02\text{ms}$). Excitation profiles were acquired as described above, altering a few parameters to shorten the acquisition ($TR = 60\text{ms}$, $\alpha = 10^\circ$).

RESULTS. As shown in Fig. 2, freq offsets alter VERSE TONE excitation profiles: TONE ramp (lower edge divided by higher edge) increases with the offset (-200Hz : 74%; 0Hz : 60%; $+200\text{Hz}$: 45%), slab profile center is shifted by up to $4.8\mu\text{m}/\text{Hz}$ (about twice the corresponding shift with non-VERSE TONE) and side lobe amplitude increases. Slice profile measurements in phantoms reproduced theoretical simulations (Fig. 3). The deviations are less than 2.5% in slice and less than 3.5% within the sidelobes. In-vivo excitation profiles are in good agreement with simulations, close to ideal profile when ΔB_0 is low (ROI1, Fig. 4-5). The distortions measured in the frontal lobe (ROI2) with local $\Delta B_0 \geq 400\text{Hz}$ are also consistent with simulations. With regards to RF power reduction, SAR was reduced to 46% when using VERSE pulses compared to the original pulses.

DISCUSSION. An inherent limitation of VERSE pulses is the sensitivity of their excitation profiles to ΔB_0 [4]. Additional challenges occur with VERSE in TONE pulses at 7Tesla because ΔB_0 offsets are greater, and altering the slope of TONE RF pulses affects vessel signal in TOF as a function of blood velocity. These results point towards some elements to consider when using VERSE for SAR management in TOF at 7T: 1) a good B_0 shim should be obtained. In our experience, simply running a few B_0 shim iterations substantially improves residual B_0 field maps. 2) fat-water chemical shift ($\sim 1\text{ kHz}$ at 7T) cannot be avoided, so that VERSE RF pulses will behave on the fat as in a large ΔB_0 and a corresponding shift of excitation slab center will occur for the fat (see Fig. 2). In a 3D acquisition this results in fat signal from skin aliased along the slab excitation axis. This may condition optimal slab positioning for TOF at 7T. Besides these points, reducing the slope of TONE pulses, or using a flat profile, also attenuates the negative impact of B_0 on VERSE profiles. Using higher values than 30% for κ would also reduce the VERSE sensitivity to ΔB_0 variations, to the cost of a lesser reduction on SAR levels.

CONCLUSION. VERSE is an elegant and efficient RF pulse technique allowing for substantial SAR reduction. Our results show that caution should be taken when applying this technique at 7T, especially with ramp RF pulses because of large ΔB_0 and large fat-water chemical shift. However, a variety of methods and tradeoff can be used to mitigate these negative effect in order to benefit from SAR reduction with VERSE at high field.

Acknowledgements: DFG grant SCHM 2671/1-1, BTRC grant P41 - RR008079, KECK Foundation. **REFERENCES** [1] Kang et al. MRM 2009;61, 136-144; [2] Zwanenburg et al. JMRI 2008;28:1519-1526 [3] Maderwald et al. MAGMA 2008;21:159-167; [4] Conolly et al. J Magn Reson 1988;78:440-477;

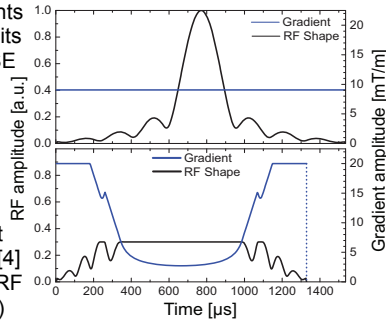


Fig. 1: Gradient and RF shape of TONE (top) and VERSE-TONE (bottom) pulses

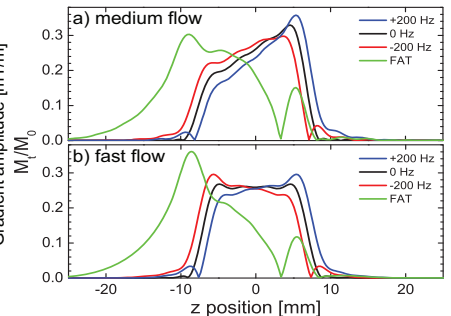


Fig. 2: transverse magnetization profile at different offset frequencies for VERSE RF pulses a) with TONE and b) without TONE.

By compressing low amplitude RF pulse segments (i.e. the sidelobes), a resulting pulse duration of 1.33 ms was achieved. **Simulations.** Excitation profiles were simulated with VERSE TONE pulses in Matlab (The MathWorks, Natick, USA) based on Bloch equations. Frequency offsets ($\pm 200\text{Hz}$) were introduced to evaluate the impact of susceptibility induced ΔB_0 . Offsets of -1000 Hz were used to evaluate water-fat chemical shift impact. Standard RF pulses (non TONE) were simulated for comparison. **Excitation profile.** Excitation profiles were measured in a phantom using an acquisition FOV along the slice direction 4 times larger than the excitation slab thickness. Imaging parameters were $TR/TE = 100\text{ms}/3.5\text{ms}$, $\alpha = 15\text{deg}$, slab/slice thickness: $16\text{mm}/0.5\text{mm}$, Matrix: $64 \times 64 \times 128$, $BW = 300\text{Hz/Px}$. To remove Receive B1 profile, $T2^*$ and Transmit B1 profile, these profiles were normalized with a 3D dataset acquired with same parameters but with a nonselective excitation (T_1 bias was minimal given the small flip angle). Residual timing errors between gradient and RF pulses were eliminated in calibration sessions. For in vivo measurements B_0 shimming was first performed with a single iteration and a field map was acquired ($TE/2 = 5.00/6.02\text{ms}$). Excitation profiles were acquired as described above, altering a few parameters to shorten the acquisition ($TR = 60\text{ms}$, $\alpha = 10^\circ$).

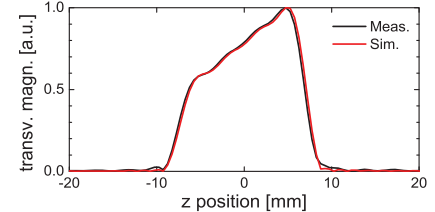


Fig. 3: simulated and measured excitation profile in a phantom

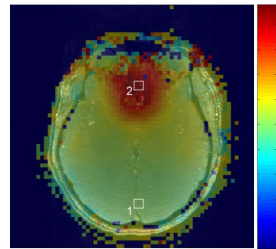


Fig. 4: fieldmap through the center of the slab ($z=0$, cp. Fig. 4)

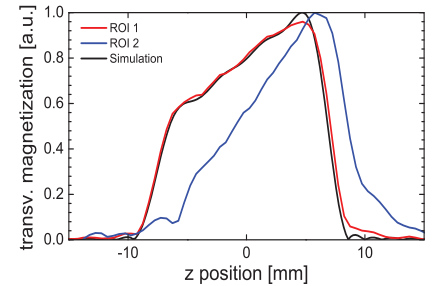


Fig. 5: measured and simulated excitation profile in vivo. The ROIs are marked in fig. 3